



**Tsang, Kwun Sing and Ion, William and Blackwell, Paul and English, Martin (2018) Industrial validation of strain in cold roll forming of UHSS. Procedia Manufacturing, 15. pp. 788-795. ISSN 2351-9789 , <http://dx.doi.org/10.1016/j.promfg.2018.07.322>**

This version is available at <https://strathprints.strath.ac.uk/65256/>

**Strathprints** is designed to allow users to access the research output of the University of Strathclyde. Unless otherwise explicitly stated on the manuscript, Copyright © and Moral Rights for the papers on this site are retained by the individual authors and/or other copyright owners. Please check the manuscript for details of any other licences that may have been applied. You may not engage in further distribution of the material for any profitmaking activities or any commercial gain. You may freely distribute both the url (<https://strathprints.strath.ac.uk/>) and the content of this paper for research or private study, educational, or not-for-profit purposes without prior permission or charge.

Any correspondence concerning this service should be sent to the Strathprints administrator: [strathprints@strath.ac.uk](mailto:strathprints@strath.ac.uk)

The Strathprints institutional repository (<https://strathprints.strath.ac.uk>) is a digital archive of University of Strathclyde research outputs. It has been developed to disseminate open access research outputs, expose data about those outputs, and enable the management and persistent access to Strathclyde's intellectual output.

17th International Conference on Metal Forming, Metal Forming 2018, 16-19 September 2018,  
Toyohashi, Japan

## Industrial validation of strain in cold roll forming of UHSS

Kwun Sing Tsang<sup>a,\*</sup>, William Ion<sup>a</sup>, Paul Blackwell<sup>a</sup>, Martin English<sup>b</sup>

<sup>a</sup>*Department of Design, Manufacture and Engineering Management, University of Strathclyde, 75 Montrose Street, Glasgow G1 1XJ, UK*

<sup>b</sup>*Hadley Group, Downing Street, Smethwick, Birmingham B66 2PA, UK*

---

### Abstract

Cold roll forming is a highly productive sheet metal forming process capable of producing an exceptional range of profile geometries. Over the last few years customers have increased the demand for high value components, through the specification of complex profiles, tighter tolerances and/or use of high strength materials. In particular, there has been a high interest by the automotive industry in utilising ultra-high strength steels (UHSSs) within the roll forming process. These steels are ideal for the forming of lightweight products, which possess increased material performance when compared to traditional low strength steels. The industry's attraction towards the roll forming process may be due to the increased deformation capabilities it can provide and due to the formability limitations of UHSS when using traditional stamping or press braking processes. This investigation aimed to determine an appropriate approach to simulating the cold roll forming process using UHSSs for future industrial applications. Currently a large volume of research can be found on the material characterisation and formability of UHSS using traditional processes. While the interest in roll forming is rapidly increasing over time, there remains a large research gap in this field. Hence, a dual phase steel (DP1000) and complex phase steel (CP1000) provided by TATA Steel were analysed using a five pass roll forming assembly to form the following two profiles: (a) V-section; and (b) flat strip with rib feature. The principal strains along the outer radius of each specimen were analysed using a GOM Argus photogrammetry system. A circle grid analysis was the method used to complete these measurements. The strain analyses were compared with corresponding strains along the surface of the finite element (FE) analysis model results. The non-linear FE simulations were carried out using COPRA® FEA RF 2017. Correlations in the results were achieved, setting a foundation for further investigations on the formability of UHSSs.

© 2018 The Authors. Published by Elsevier B.V.

Peer-review under responsibility of the scientific committee of the 17th International Conference on Metal Forming.

---

\* Corresponding author. Tel.: +44-141-548-2091.

E-mail address: [kwun.tsang@strath.ac.uk](mailto:kwun.tsang@strath.ac.uk)

**Keywords:** Cold roll forming; Sheet metal; Finite element analysis; Ultra-high strength steel

## 1. Introduction

Cold roll forming is an incremental sheet metal forming process, which offers a wide range of advantages when compared to alternative forming processes such as stamping or press forming. This process consists of forming coiled sheet metal through a series of rolls in tandem to achieve a desired cross section as shown in Fig. 1. This process is desirable when high volume and high productivity is required. Low tooling costs are associated due to the ability to incorporate in line processes and use of the same tooling when varied length products are specified.

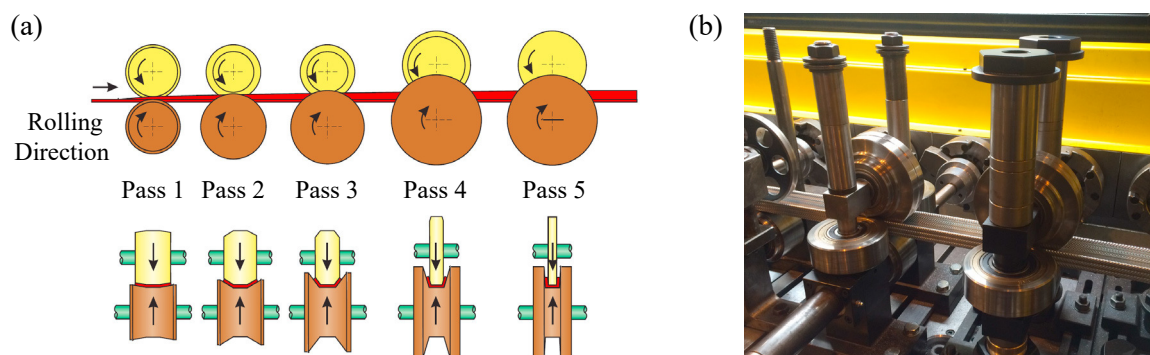


Fig. 1. (a) Schematic [1] and (b) image of roll forming process.

An empirical process is still currently widely adopted by roll designers during the design of new tooling [2, 3]. This is a challenge as there are no scientific methodologies readily available to carry out this task and the success of a product relies on the experience and intuition of highly skilled roll designers. However, designers now have the opportunity of virtually optimising forming strategies and investigating the effects of certain parameter changes within the roll forming process with the use of finite element (FE) analysis. This can significantly reduce the associated costs due to a decrease in tool modifications and/or scrapping of material.

The automotive industry currently has a high interest in utilising UHSSs within the roll forming process. These steels are ideal for the forming of lightweight products, which possess increased material performance when compared to traditional low strength steels [4]. Typical tensile strengths of UHSSs can range from 1000-1600 MPa and is achieved through the introduction of different phases to the materials microstructure, e.g. martensite, retained austenite, bainite and ferrite. Note that the strength and ductility properties of UHSS are inversely proportional and desired material performances can be achieved by changes in the microstructure, i.e. increase strength by increasing the percentage of martensite or bainite; or increase ductility by increasing the percentage of ferrite [5]. The industry's attraction towards the roll forming process may be due to its increased deformation capabilities and the formability limitations of UHSS when using traditional stamping or press braking processes.

A common challenge that faces the designer is satisfying product specifications. These specifications may include dimensional accuracy and product performance. This challenge is increased when UHSS materials are introduced and the material behavior and characteristics during the roll forming process is unknown.

The fundamental deformation types have been identified in roll forming as the following: longitudinal strain; longitudinal and transversal bending; and shear in the strip plane [6]. In roll forming it is the transversal bending, which is the desired deformation. However, little knowledge is readily available on the limitations of this deformation for UHSS. Fortunately this aspect can be studied through FE.

Therefore the objective of this paper is to determine the capability of using FE to model the forming of UHSSs within the roll forming process. As roll forming is a complex multi-stage process, a number of simplifications and assumptions will need to be incorporated into the FE model and validated against experimental data. Correlation in results will validate this process for future analyses when determining the formability and failure analysis of UHSS.



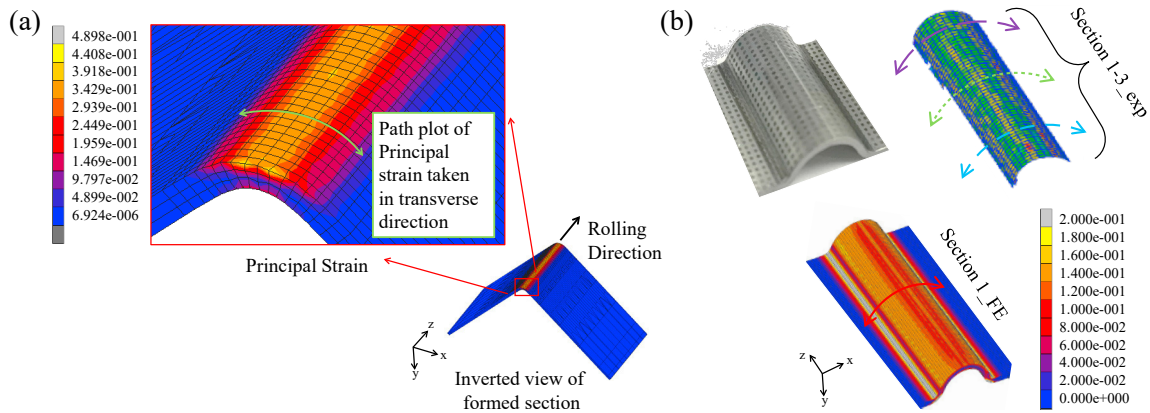


Fig. 3. Path plot measured across outside radius; (a) profile 1; and (b) profile 2 – exp. vs. FE.

### 2.1. Mesh optimisation

Profile 1 was considered in this study for the mesh optimisation analysis. Five mesh models were considered as illustrated in Fig. 4. Note that certain sections of the profile were categorised into one of two features: straight and radial elements. For this study it was only the radial elements that were of interest, hence, the mesh optimisation process focused on the aspect ratio of these elements. For each mesh model, the number of elements were increased along each direction, i.e. the transverse, thickness and longitudinal direction as defined later in Table 3. The peak principal strain was considered along the centre of the profile and compared with the experimental data. Note that the strip material was modelled with a total length of 567 mm, however, only a section of the model was modified with increasing elements to avoid long computational time. The modified length of the strip was approximately 50 mm in length along the longitudinal direction. This optimised mesh was later adopted for the analysis of profile 2.

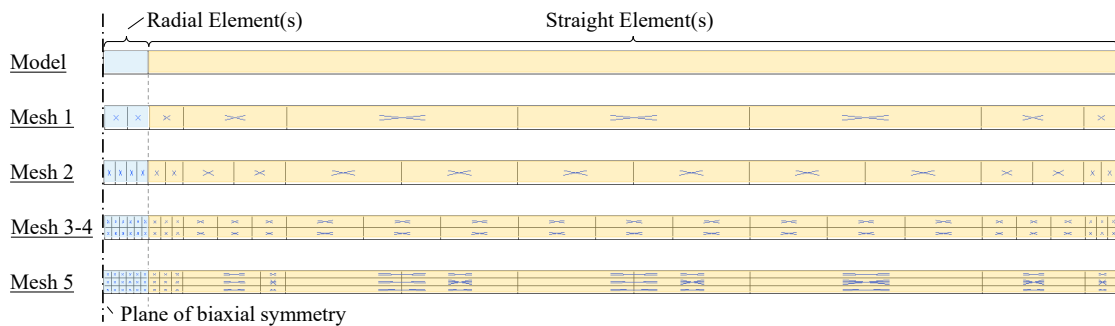


Fig. 4. Mesh optimisation models 1-5 (cross section).

### 2.2. Material model optimisation

The material properties implemented into the FE simulation was investigated in order to determine an appropriate material model. This optimisation process considered both the correlation of the simulated results data with experimental results, and the viability of using the selected method in an industrial application. Tensile tests were carried out by Warwick Manufacturing Group (WMG) as part of the EPSRC project – EP/M014096/1 on the DP1000 material, considering the specimen sample orientations set at 0, 45 and 90° with respect to the rolling direction. The stress strain curve results were collected and are presented in Fig. 5. An average of the yield strength was determined as 722 MPa and the average tensile strength as 1162 MPa. The Young's modulus was assumed to be 205 GPa with a Poisson's ratio of 0.3. Using these values, COPRA® FEA RF generated a fitted stress strain curve using the Swift power law. This generated COPRA flow curve is presented in Fig. 5 along with the tensile results.

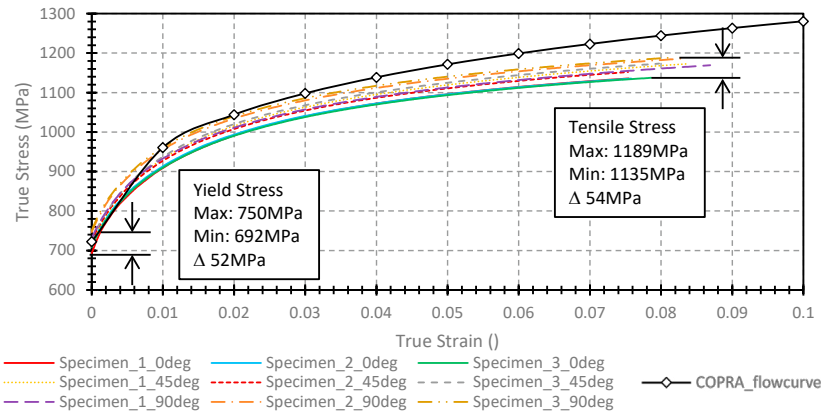


Fig. 5. DP1000 stress-strain curve – experimental vs. COPRA curve.

It was observed that the maximum deviation of all the measured yield stress and tensile stresses were 52 MPa and 54 MPa, respectively. These tests suggests isotropic material properties can be assumed for the studied material and modelled using the most widely used von Mises yield criterion. However, according to the MARC Theory and User Information [11], complete isotropy is achieved when the following two conditions are met,  $\sigma_0 = \sigma_{45} = \sigma_{90}$  and  $r_0 = r_{45} = r_{90} = 1$ . The yield stresses acting in the three directions relative to the rolling direction (0, 45 and 90°) are shown to have a deviation up to 52 MPa, Fig. 5, and approximately a ratio of 1:1 when compared to yield in the rolling direction,  $\sigma_0$ , Table 1. The anisotropy value, also known as the plastic strain ratio,  $r$ , was measured and presented in Table 1. Due to the deviation between these values and due to them not being equal to 1, both the von Mises and Hill (1948) yield criterion were studied. Both the material flow curve obtained from tensile tests and the COPRA generated flow curve were studied. The four material model set ups are shown in Table 2.

Table 1. Material input parameters – DP1000.

Yield stress (MPa)	Yield stress relative to $\sigma_0$	Plastic strain ratio
$\sigma_0$ 704	$\sigma_0 / \sigma_0$ 1.0000	$r_0$ 0.35894
$\sigma_{45}$ 720	$\sigma_{45} / \sigma_0$ 1.0227	$r_{45}$ 0.51901
$\sigma_{90}$ 743	$\sigma_{90} / \sigma_0$ 1.0554	$r_{90}$ 0.45923

Table 2. Material model analysis.

Material Model	Flow Curve	Yield Criterion
1	COPRA	von Mises
2	COPRA	Hill (1948)
3	Experimental	von Mises
4	Experimental	Hill (1948)

### 3. Experimental analysis

A standard roll forming mill was used in this study to carry out the forming process of the two defined sections. The mill configuration is equal to that defined in the numerical model set up, Fig. 2 with the exception of the strip translation. During the physical forming process, the forming rolls were fixed in position with the strip material driven from one pass to the next due to contact between the material and roll tools. Note that only the bottom rolls were subject to a drive motor to provide rotation. The two sections were analysed after the forming process with particular interest in the development of strain fields where bending occurs. This data was required to complete the validation process of the FE simulations.

Prior to the forming process, the flat strip material was prepared using an electrochemical etching method to apply a uniformly distributed pattern of dots on the surface of the material. This etched pattern was applied with dot diameters of 0.5 mm and a spacing of 1 mm in each direction, Fig. 6. Once the material was subjected to the forming



process, analyses was carried out to determine the developed strains using a GOM Argus photogrammetry system. A circle grid analysis was the method used to complete these measurements.

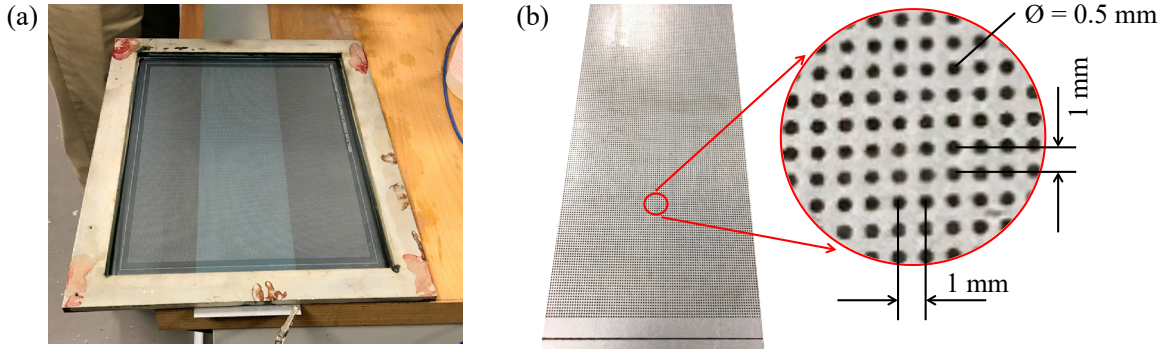


Fig. 6. (a) Electrochemical etching method; (b) etch definition.

#### 4. Results and discussion

Table 3 presents the mesh optimization analysis results, which includes the element aspect ratio and peak principal strains measured along the centre of the profile for both FE and experimental trials. It can be seen that relatively large elements as defined in mesh 1 produces promising results when compared with experimental data. However, due to the small number of elements across the radial feature a poor representation of the strain path is captured. Taking this into consideration, mesh 5 was selected for the remaining analyses in this study.

Table 3. Mesh optimisation.

Mesh	No. elements across		Element aspect ratio			Peak principal strain ( )	
	Thickness	Width	W	H	L	FE	Exp
1	1	2	1.17	1.20	3.61	0.3275	Between 0.3093 and 0.3300
2	1	4	0.59	1.20	1.81	0.3851	
3	2	6	0.39	0.60	1.20	0.3042	
4	2	6	0.39	0.60	0.60	0.2948	
5	3	6	0.39	0.40	0.40	0.3181	

An analysis into the material model optimisation was carried out using the selected mesh 5. The results of the four material models as defined in the matrix in Table 2 are presented in Fig. 7 (a). The strain path along the radial feature is plotted and compared to physical data. It can be observed that the physical data measures a peak principal strain along the transverse direction between 0.3093 and 0.33. When compared to the simulated results, material model 1 shows the best agreement. Based on these results, the DP1000 UHSS material can be considered to behave as an isotropic material and modeled using a von Mises yield criterion. It can be observed that the COPRA flow curve generates a conservative strain path when compared to experimental input. The discrepancies between the results aren't significant but may be critical when the material is subjected to increased angles of bend or tighter radii. Considering the same strain curves, it can be observed that the width of the simulated curves are narrower when compared to the experimental data. The reason for this is unclear. However, the experimental data is subject to a 1% error which may be the underlying reason for this. For the purpose of this study this is not considered important but may be more influential in future work when springback is considered.

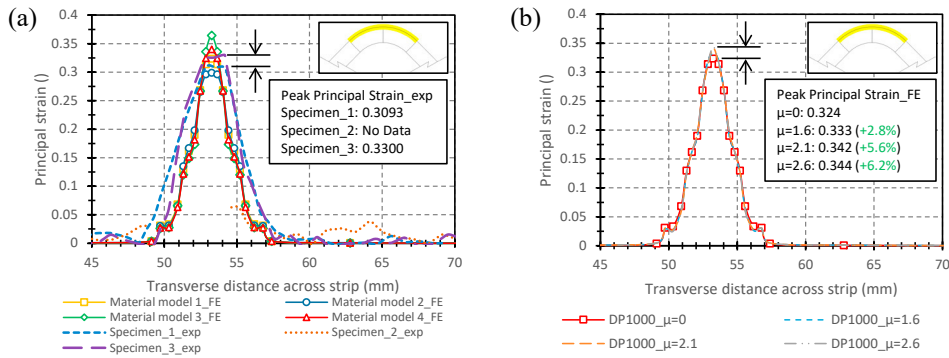


Fig. 7. Principal strains along transverse direction; (a) material model analysis; (b) friction analysis.

Considering this optimised mesh and material model, three further analyses were carried out as follows:

- Profile 1 using the defined DP1000 to consider the effect of friction;
- Profile 1 using a complex phase steel, CP1000; and
- Profile 2 using the defined DP1000.

The effect of friction was investigated by modifying the current model, in which the roll tools were subjected to a rotational force to drive the material from one pass to the next due to the contact between material and tooling. Three friction coefficient values were investigated:  $\mu = 0.21$  based on industrial experience;  $\mu = 0.16$  (low); and  $\mu = 0.26$  (high). The effect of friction on the measured principal strains are shown in Fig. 7 (b) with deviations ranging between 2.8% and 6.2%. These results indicate that a change in the friction coefficient appears not to have a significant effect on the developed principal strains during the roll forming process.

It can be seen in Fig. 8 (a) the flow curve implemented into the FE analysis for the CP1000 material. The curve was generated using COPRA® FEA RF as carried out previously for the DP1000 material. Repeating the analysis with the amended material, good correlation is achieved between the measured principal strains from FE and experimental data, Fig. 8 (b).

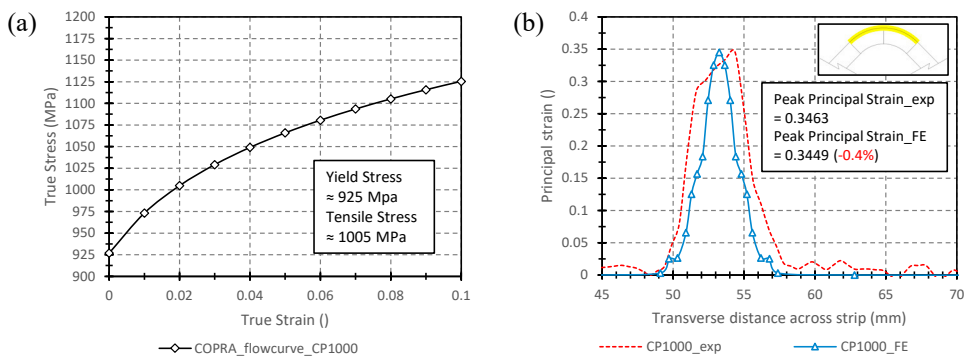


Fig. 8. (a) CP1000 stress strain curve; and (b) Profile 1 – principal strain analysis – CP1000.

Fig. 9 presents the principal strains for profile 2, comparing FE and experimental results. These strains are measured across an increased arc length due to the increased radius, i.e. approximately two times the radius to that in profile 1. It can be seen that the current FE analysis is capable of producing a valid strain profile across the surface of a roll formed part using UHSS and can be applied to further studies. Note that both profile 1 and profile 2 were used to represent a simple forming process and are not representative of the more complex geometries required.



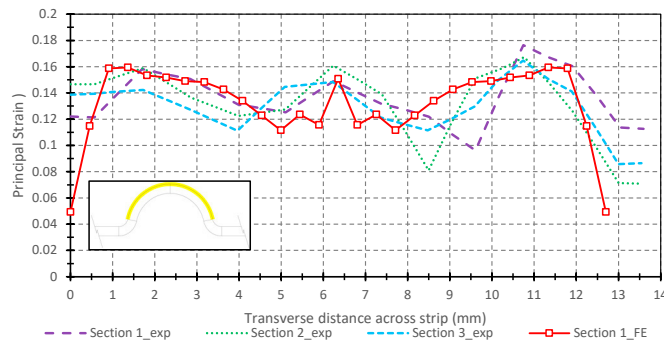


Fig. 9. Profile 2: principal strain analysis - DP1000.

## 5. Conclusion

This investigation considers the cold roll forming process using a DP1000 and CP1000 steel, provided by TATA Steel on behalf of the EPSRC project – EP/M014096/1. The experimental process consisted of roll forming the following two profiles: (a) a V-section; and (b) a flat strip with a rib feature along the centre. The strain analysis measurements were carried out by WMG as part of the referenced EPSRC project. Experimental data was used to validate FE data, in which COPRA® FEA RF 2017 was used as the nonlinear FE software. The description of the pre- and post-processing of the numerical simulation set up is included in this study. The results obtained through this study consisted of the principal strains acting in the transverse direction of the profile. Good correlation was achieved between FE and experimental data for simple profiles. Hence, future work shall include the analysis of alternative UHSS materials and/or more complex representative geometries for the automotive industry, using increased angles of bend and/or reduced radii. These further studies will investigate the formability of UHSS, springback and failure analysis in order to develop design forming limitations for an industrial application.

## Acknowledgements

The author would like to express his gratitude to Hadley Group for the continuous support and contributions towards this work and overall research being conducted on behalf of the author's Engineering Doctorate programme with University of Strathclyde. Special thanks to be extended to WMG for their contributions in this work.

## References

- [1] G.T. Halmos, Roll forming handbook, CRC Press, (2005).
- [2] N. Duggal, M.A. Ahmetoglu, G.L. Kinzel, T. Altan, Computer aided simulation of cold roll forming – a computer program for simple section profiles, *Journal of Materials Processing Technology*, 59 (1996) 41–48.
- [3] S. Hong, S. Lee, N. Kim, A parametric study on forming length in roll forming, *Journal of Materials Processing Technology*, 113 (2001) 774–778.
- [4] J.Y. Koo, G. Thomas, Design of duplex low carbon steels for improved strength: weight applications, Symposium on Modern Developments in HSLA Formable Steels, Chicago, IL, (1977).
- [5] M. Sarwar, R. Priestner, Influence of ferrite-martensite microstructural morphology on tensile properties of dual-phase steel, *Journal of Materials Science*, 31 (1996) 2091–2095.
- [6] S.M. Panton, S.D. Zhu, J.L. Duncan, Fundamental deformation types and sectional properties in roll forming, *International Journal of Mechanical Sciences*, 38 (1994) 725–735.
- [7] F. Heizlitz, H. Livatyali, M.A. Ahmetoglu, G.L. Kinzel, T. Altan, Simulation of roll forming process with the 3-D FEM code PAM-STAMP, *Journal of Materials Processing Technology*, 59 (1996) 59–67.
- [8] J.J. Sheu, Simulation and optimization of the cold roll forming process, *Proceedings of the 8<sup>th</sup> International Conference on Numerical Methods in Industrial Forming Processes*, 712 (2004) 452–457.
- [9] Q.V. Bui, J.P. Ponthot, Numerical simulation of cold roll-forming processes, *Journal of Materials Processing Technology*, 202 (2008) 275–282.
- [10] MARC®2014, Volume b: Element library, (2014) 71–72.
- [11] MARC®2014, Volume a: Theory and user information, (2014) 471–475.